ChemComm

Accepted Manuscript

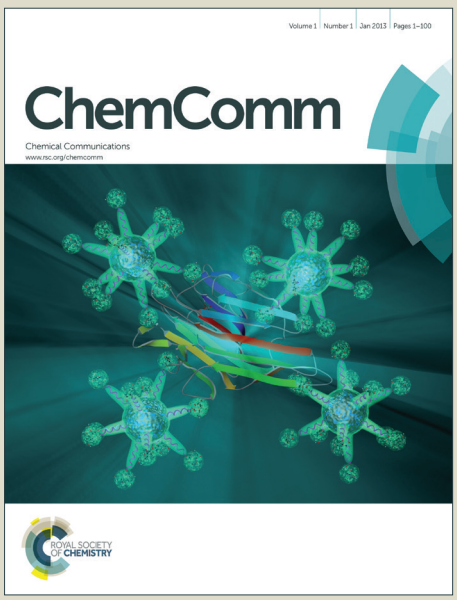

ROYAL SOCIETY OF CHEMISTRY

www.rsc.org/chemcomm

Journal Name

RSCPublishing

COMMUNICATION

Coordination Polymers for Catalysis: Enhancement of Catalytic Activity through Hierarchical Structuring

Cite this: DOI: 10.1039/x0xx00000x

Fan-Xing Bu, Ming Hu, Li Xu, Qi Meng, Gui-Yun Mao, Dong-Mei Jiang and Ji-Sen Jiang*

Received 00th January 2012,
Accepted 00th January 2012

DOI: 10.1039/x0xx00000x

www.rsc.org/

We utilized a novel strategy, hierarchical structuring, to enhance the catalytic activity of coordination polymers. Hierarchical Prussian white crystals with hollow structures and kinked surfaces were synthesized by using self-aggregation and etching strategy. The hierarchical structure enhanced the catalytic activity of Prussian white in degradation of methylene blue than the non-hierarchical Prussian white crystals significantly.

Coordination polymers, including metal-organic frameworks (MOFs) or porous coordination polymers (PCPs), are hybrid inorganic-organic materials formed by self-assembly of metal ions (or clusters) and ligands.[1] Their adjustable structures and compositions drive them to show great promise in wide applications, such as gas storage, separation and sensing.[2] Especially, coordination polymers have been recognized as potential catalysts in heterogeneous catalysis owing to the adjustable metallic and organic components, and the flexible porous structure.[3] For example, MOFs containing catalytically active metal ions or clusters, functional organic linkers, or loading with active catalysts have been fabricated and used in heterogeneous catalysis.[4] However，in order to obtain catalysts with excellent property, most of the related research focused on the exploration of new coordination polymers with new compositions and crystal structures, or introducing excellent nano-catalysts into their intrinsic pores.

It is well-known that nano-/microstructures of catalysts are important factors in influencing the catalytic activity. Nano-/microstructured catalysts generally have higher specific surface area and more active sites, which are needed for enhancing the activity of catalysts.[5] Therefore, it is interesting to investigate the performance of coordination polymers with controlled nano-/microstructures in catalysis. However, little attention has been paid on the influence of nano-/microstructures of coordination polymers.

To design optimized nano-/microstructures of coordination polymers in catalysis, previous study has been referred.[6] Extensive study on noble metals and metal oxides catalysts suggested that hollow structures and kinked surfaces worked very well in improving the performance of catalysts.[6] The hollow structures offer high surface-to-volume ratio, thus enlarge the exposed surface of catalysts.[6a-f] The kinked surfaces provide more active sites compared to smooth surfaces.[6g-i] Therefore, materials with hierarchical structure, which can combine both hollow structures and kinked surfaces, can be expected as a good choice for catalysis.

To synthesize coordination polymers with hierarchical structures, controlled crystallization is critical but challenging. Owing to the lack of knowledge about crystallization habit of coordination polymers, the morphology-controlled synthesis is not as successful as noble metals and metal oxides.[7] It has been illustrated that the hierarchical structuring of nano-/microstructured coordination polymers mainly relied on utilization of non-classical crystallization process.[8] Well-control on self-assembly of preformed clusters or nanoparticles as well as further treatment, such as etching or aging,[8a, 8b] could lead to coordination polymers with well-defined nano-/microstructures. As a proof of concept, we employed the non-classical crystallization and external etching strategy to fabricate coordination polymer with hierarchical structure composed by hollow structure and kinked surface both. Here, Prussian white (PW) was selected as a typical coordination polymer, which was formed by assembly of Fe ions and CN bridges.[9] The shape-dependent catalytic performance of PW was investigated. The hierarchical structure did enhance the catalytic activity of PW for decomposition of methylene blue (MB).

In a typical synthesis, hierarchical PW crystals were prepared by solvothermal treatment of potassium ferrocyanide and benzoic acid in the mixture of water/ethanol (please see the details in ESI†). X-ray diffraction (XRD) profile (Fig. S1) demonstrates that the obtained products are PW with high purity. All of these peaks can be assigned to monoclinic lattice (JCPDS 51-1896).[9] Fourier transform infrared spectroscopy (FTIR) (Fig. S2) and Mössbauer spectroscopy (Fig. S3) were used to further confirm the composition of the products. The strong absorption peaks at 2037 cm^{-1} and 2073 cm^{-1} are characteristic CN stretching absorption bands of PW.[10] The absorption band at around 594 cm^{-1} is due to the structure of Fe^{II}-CN-Fe^{II} linkage.[11] The Mössbauer spectrum of the product contains a singlet absorption peak (the isomer shift is -0.1 mm/s) and a doublet absorption peak (the isomer shift is 1.11 mm/s and the quadrupole splitting is 1.52 mm/s), which are attributed to the low spin Fe^{II} and the high spin Fe^{II}, respectively.[9] The stability of PW in air was confirmed by the XRD profile and Mössbauer spectrum of the product exposed in air for four months (Fig. S4 and Fig. S5).

Both the XRD pattern and the Mössbauer spectrum were the same as the fresh PW sample, suggesting that the PW crystals obtained in this work were quite stable.

The morphology of the obtained hierarchical PW was examined by electron microscopy. Field emission scanning electron microscope (FESEM) image shows the typical morphology of the PW crystals (Fig. 1a). The holes and step-like surfaces are observed on each of the six faces, suggesting that the crystals are of hierarchical structures with hollow structure and kinked surfaces. A low magnification FESEM image (Fig. S6) clearly reveals high yield of the hierarchical PW crystals. The X-shape morphology in a transmission electron microscopy (TEM) picture (Fig. 1b) taken from a crystal confirms the existence of cavities and step-like surfaces as well, which further verifies that the hierarchical structure is the combination of hollow structure and kinked surfaces.

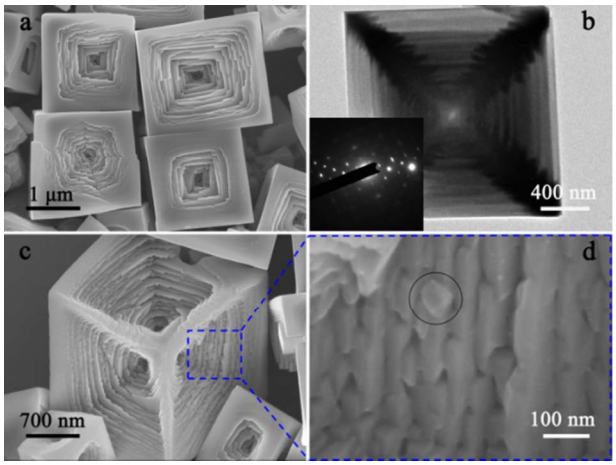

Fig. 1 (a) FESEM image of sample prepared following a typical procedure. (b) TEM, (c) and (d) High magnification FESEM images of a single hierarchical PW crystals. (inset: selected area electron diffraction (SAED) pattern taken from the edge section).

The hierarchical PW crystals are of relatively ordered crystallographic orientation as suggested by SAED pattern taken from a single crystal. The periodic diffraction spots are shown in the inset of Fig. 1b, indicating a single-crystal-like electron diffraction behavior. To further investigate the kinked surfaces, a part of the crystal was shown in Fig. 1c and Fig 1d. It can be observed that the kinked surfaces are composed by nanocrystals with quasi-ordered orientation. In addition, significant defects, such as gaps between different steps and gaps among the same steps, are observed. In combination of the single-crystal-like electron diffraction behavior as well as the rough surfaces, the hierarchical PW crystals belong to mesocrystals. Mesocrystals are one kind of superstructures formed by self-assembly of nanocrystals in ordered ways, often showing single-crystal-like electron diffraction behavior.[12] They are usually obtained by non-classical crystallization route, for example, bottom-up self-assembly. This unique crystallization style could make them have rough surfaces with large amount of exposed sites, and thus high catalytic activity.[13]

The crystallization of PW highly depends on the supersaturation of PW before and /or during the nucleation and/or growth process of PW. High supersaturation degree was proved to be essential for the formation of hierarchical mesocrystals.[14] In our case, the formation of PW mesocrystals is strongly influenced by the reaction conditions, such as the concentration of reagents and the polarity of solvents. For instance, when we decreased the concentration of potassium ferrocyanide, the product of $[Fe(CN)_6]^{4-}$ and Fe^{2+} decreased,[8a, 9] leading to reduction of the supersaturation degree of PW, thus only convex cuboids (Fig. S7) were the dominant products. When water was partially replaced by ethanol, the polarity of the solvent was decreased, hindering the dissociation of H^+ from benzoic acid.[15] Then, the decomposition of potassium ferrocyanide was slow down, inducing a lower surpersaturation degree of PW, and resulting in cuboids (Fig. S8). This result is in agreement with the formation of the calcite mesocrystals with similar structure.[16] Therefore, we can see the generation of the hierarchical PW mesocrystals is quite similar to other biomineral systems.

To illustrate the formation mechanism of the hierarchical PW mesocrystals, time-dependent experiments were carried. FESEM images of the products collected at an early reaction stages were shown in Fig. S9. Products at 30 min are spherical particles with sizes ranging from 200 nm to 800 nm (Fig. S9a). The surface of these spherical particles is very rough (Fig. S9b), indicating that these particles were probably formed by self-assembly of smaller nanoparticles. When the reaction time was prolonged to 1h, the sizes of particles increased, varying from 500 nm to 1.5 μm (Fig. S9c). Furthermore, the spherical particles formed at 30 min have been transformed into aggregations of particles. These aggregations are of rough interior and smooth exterior surfaces, which can be demonstrated by some broken aggregations (inset in Fig. S9c). This observation reveals that these aggregations probably come from the single spheres formed at 30 min. Magnified FESEM image (Fig. S9d) indicates that the particles do not have holes and kinked surfaces at this stage. With the further increase of the reaction time (2 h), cavities and kinked surfaces were created in most of the particles (Fig. S9e and Fig. S9f). As the reaction time was prolonged to 3 h, more hierarchical particles with significant step-like structures and holes (Fig. S9g and Fig. S9h) were obtained. At this time, some irregular nanoparticles similar to those particles found in the resulted products as indicated by circle (Fig. 1d) were also seen on the hierarchical surface of the PW crystals (Fig. S9h). It is highly possible that the nanoparticles were once the parts of some stairs, and departed from the stairs. The fusion of nanoparticles might also take place, because the steps in this stage and the following periods were very large and smooth.

According to the above analysis, the formation mechanism of the hierarchical PW crystals was proposed (Fig. 2). At first, large amounts of nanoparticles were formed rapidly due to high supersaturation degree at the initial stage (Fig. 2a). Nanoparticles are easily aggregated owing to the high surface energy (Fig. 2b).[12b, 17] Subsequently, the spherical particles were fused together into aggregations with cubic corners covering their surface (Fig. 2c). Along with the prolonging of reaction duration, external etching occurred while growth continued (Fig. 2d). Because the particles-based non-classical crystallization dominated the growth process, defects existed between the aggregated nanoparticles. The defects were easily to be etched by H^+ disassociated from benzoic acid, leading to step-like detachment of nanoparticles.[6c, 6d, 8a, 8c, 18] Finally, hierarchical crystals could be formed.

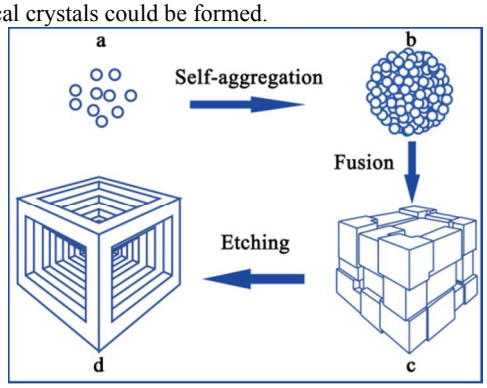

Fig. 2 Schematic illustration of the formation process of hierarchical PW crystals.

The hierarchical PW crystals combine the hollow structure and kinked surface together, which motivates us to investigate their catalytic performance. Nowadays, the ever-growing contamination of water has attracted a great deal of attention. Advanced oxidation processes[19] based on reactive oxygen species generated by Fenton catalysts have been widely used to remove the toxic organic compounds in water. Fenton-like heterogeneous catalysts based on iron-based compounds[20] are among the most attractive catalysts, due to their high stability and the facility to separate them. As a reduced form of Prussian blue (PB), PW has strong reducibility and had been explored in electrochemical catalysis for proton reduction[21] and sensing of oxidants.[22] Therefore, PW is a suitable electron donor and holds great potential in application as Fenton-like catalysts.

The hierarchical PW crystals were exploited as Fenton-like catalyst for the degradation of MB. MB was selected as a model target because it is one of the most commonly used dyes in various industries and had been widely used as probe compound for the advanced oxidation process. For comparison, cubic PW crystals without hierarchical structure (Fig. S10) were used. Almost no MB (only about 4%) was degraded in the absence of PW (Fig. S11), which demonstrated that PW was indispensable for degradation of MB. Surprisingly, the degradation of MB was largely enhanced by using hierarchical PW crystals as catalysts, as shown in Fig. 3a and Fig. 3b. Compared to cubic PW crystals (less than 24 % MB was decolorized after 5 min), more than three times of MB (73.9 %) was decolorized at 5 min for hierarchical PW crystals. Moreover, all of the MB was removed in the presence of hierarchical PW crystals after 25 min while only less than 43 % MB was degraded by cubic PW crystals. The possible reasons for the high performance of hierarchical PW can be described as two points. Firstly, the hierarchical architecture can provide more active surface, such as steps, kinks, corners and edges, causing rapid degradation of MB at the initial stage.[6g, 6i] Secondly, the nanoscale size of its building blocks and hollow structure enlarge the specific surface area of the hierarchical PW crystals, and facilitate the mass exchange and catalysis process.[6a, 23]. According to N_2 gas sorption analysis, the Brunauer–Emmett–Teller (BET) surface area of the hierarchical PW crystals (12.0 m^2/g) is as twice as cubic PW crystals (6.0 m^2/g).

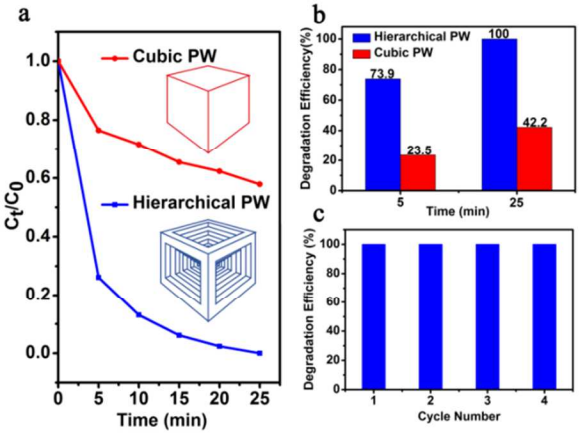

Fig. 3 (a) The time-dependent degradation curves of MB catalysed by hierarchical PW and cubic PW. (b) Comparison of catalytic activity of hierarchical PW and cubic PW in degrading MB. (c) The cyclic performance of hierarchical PW for the decolorization of MB.

To check the structure stability of the hierarchical PW crystals as catalyst, XRD and SEM measurements of the hierarchical PW crystals during one catalysis cycle were carried out. As shown in Fig. S12a, the composition of the samples underwent PW-(PW/PB)-PW transformation, indicating PW was partly oxidized into PB (JPCDS 73-0687) during the catalytic reaction and the PB was reduced back to PW after the activation process. In addition, the size, morphology and hierarchical structure of the samples (Fig. S12b and Fig. S12c) are all well-maintained, indicating the hierarchical structure is robust. In consideration of these aspects, its cyclic property was checked. As shown in Fig. 3c, the hierarchical PW crystals show excellent reusable ability, without any loss of activity after four cycles.

Conclusions

In conclusion, PW with hierarchical structures were synthesized by a one-pot solvothermal reaction. Non-classical crystallization and etching took place to realize the integration of hollow structures and kinked surfaces. By taking together the advantages of the hollow structure and kinked surfaces, we found that the performance of PW in catalysis could be enhanced significantly. The as-prepared hierarchical PW is believed to be a potential candidate as a practical catalyst for water purification. Such results offer a way to realize coordination polymers with hierarchical structures, encourage the application of coordination polymers as superior heterogeneous catalysts, and open a new way to elevate the performance of coordination polymers through hierarchical structuring.

Acknowledgments

This work was supported by the National Natural Science Foundation of China (Grant No. 21173084) and Large Instruments Open Foundation of East China Normal University.

Notes and references

Department of Physics, Center for Functional Nanomateriels and Devices, East China Normal University, Shanghai 200241, P.R. China
E-mail: jsjiang@phy.ecnu.edu.cn

† Electronic Supplementary Information (ESI) available: XRD, FTIR, Mössbauer spectrum and FESEM pictures of the PW crystals. XRD and Mössbauer spectrum of the PW crystals exposed in air for four months. FESEM images of the products obtained at varied reagents concentration and solvent ratio. FESEM images of the products obtained at different reaction times. XRD and FESEM pictures of cubic PW crystals. The time-dependent degradation curves of MB in the absence of PW. The nitrogen adsorption–desorption isotherms and the pore size distribution curves of the hierarchical and cubic PW crystals. XRD and SEM images of the hierarchical PW crystals during one catalysis cycle. See DOI: 10.1039/c000000x/

1 (a) S. Kitagawa, R. Kitaura and S. i. Noro, *Angew. Chem. Int. Ed.*, 2004, **43**, 2334; (b) H. C. Zhou, J. R. Long and O. M. Yaghi, *Chem. Rev.*, 2012, **112**, 673.

2 (a) H. Furukawa, N. Ko, Y. B. Go, N. Aratani, S. B. Choi, E. Choi, A. Ö. Yazaydin, R. Q. Snurr, M. O'Keeffe, J. Kim and O. M. Yaghi, *Science*, 2010, **329**, 424; (b) Y. Q. Lan, H. L. Jiang, S. L. Li and Q.

Xu, *Adv. Mater.*, 2011, **23**, 5015; (c) Y. Takashima, V. M. Martínez, S. Furukawa, M. Kondo, S. Shimomura, H. Uehara, M. Nakahama, K. Sugimoto and S. Kitagawa, *Nat. Comm.*, 2011, **2**, 168; (d) M. M. Wanderley, C. Wang, C. D. Wu and W. Lin, *J . Am. Chem. Soc.*, 2012, **134**, 9050.

3 (a) J. Lee, O. K. Farha, J. Roberts, K. A. Scheidt, S. T. Nguyen and J. T. Hupp, *Chem. Soc. Rev.*, 2009, **38**, 1450; (b) J. Gascon, A. Corma, F. Kapteijn and F. X. Llabrés i Xamena, *ACS Catal.*, 2013, **4**, 361; (c) L. Ma, C. Abney and W. Lin, *Chem. Soc. Rev.*, 2009, **38**, 1248.

4 (a) M. Fujita, Y. J. Kwon, S. Washizu and K. Ogura, *J . Am. Chem. Soc.*, 1994, **116**, 1151; (b) S. Hasegawa, S. Horike, R. Matsuda, S. Furukawa, K. Mochizuki, Y. Kinoshita and S. Kitagawa, *J . Am. Chem. Soc.*, 2007, **129**, 2607; (c) R. K. Totten, Y. S. Kim, M. H. Weston, O. K. Farha, J. T. Hupp and S. T. Nguyen, *J . Am. Chem. Soc.*, 2013, **135**, 11720; (d) C. Wang, K. E. deKrafft and W. Lin, *J . Am. Chem. Soc.*, 2012, **134**, 7211; (e) G. Lu, S. Li, Z. Guo, O. K. Farha, B. G. Hauser, X. Qi, Y. Wang, X. Wang, S. Han, X. Liu, J. S. DuChene, H. Zhang, Q. Zhang, X. Chen, J. Ma, S. C. J. Loo, W. D. Wei, Y. Yang, J. T. Hupp and F. Huo, *Nature Chem.*, 2012, **4**, 310; (f) Q. L. Zhu, J. Li and Q. Xu, *J . Am. Chem. Soc.*, 2013, **135**, 10210.

5 (a) N. Wang, D. Wang, M. Li, J. Shi and C. Li, *Nanoscale*, 2014, **6**, 2061; (b) M. Turner, V. B. Golovko, O. P. H. Vaughan, P. Abdulkin, A. Berenguer Murcia, M. S. Tikhov, B. F. G. Johnson and R. M. Lambert, *Nature*, 2008, **454**, 981; (c) R. Schlögl and S. B. Abd Hamid, *Angew. Chem. Int. Ed.*, 2004, **43**, 1628; (d) F. Shi, Y. Li, H. Wang and Q. Zhang, *Appl. Catal. B: Environ.*, 2012, **123–124**, 127.

6 (a) B. Y. Xia, H. B. Wu, X. Wang and X. W. Lou, *J . Am. Chem. Soc.*, 2012, **134**, 13934; (b) H. Zhang, M. Jin, H. Liu, J. Wang, M. J. Kim, D. Yang, Z. Xie, J. Liu and Y. Xia, *ACS Nano*, 2011, **5**, 8212; (c) M. Hu, S. Furukawa, R. Ohtani, H. Sukegawa, Y. Nemoto, J. Reboul, S. Kitagawa and Y. Yamauchi, *Angew. Chem. Int. Ed.*, 2012, **51**, 984; (d) M. Hu, A. A. Belik, M. Imura and Y. Yamauchi, *J . Am. Chem. Soc.*, 2012, **135**, 384; (e) H. Ataee-Esfahani, J. Liu, M. Hu, N. Miyamoto, S. Tominaka, K. C. W. Wu and Y. Yamauchi, *Small*, 2013, **9**, 1047; (f) X. Li, J. Liu, A. F. Masters, V. K. Pareek and T. Maschmeyer, *APL Mat.*, 2013, **1**, 041101; (g) B. Y. Xia, H. B. Wu, X. Wang and X. W. Lou, *Angew. Chem. Int. Ed.*, 2013, **52**, 12337; (h) H. Zhang, M. Jin, J. Wang, W. Li, P. H. C. Camargo, M. J. Kim, D. Yang, Z. Xie and Y. Xia, *J . Am. Chem. Soc.*, 2011, **133**, 6078; (i) H. Zhang, M. Jin and Y. Xia, *Angew. Chem. Int. Ed.*, 2012, **51**, 7656.

7 (a) C. M. Doherty, D. Buso, A. J. Hill, S. Furukawa, S. Kitagawa and P. Falcaro, *Acc. Chem. Res.*, 2013, **47**, 396; (b) J. Reboul, S. Furukawa, N. Horike, M. Tsotsalas, K. Hirai, H. Uehara, M. Kondo, N. Louvain, O. Sakata and S. Kitagawa, *Nature Mater.*, 2012, **11**, 717; (c) A. Umemura, S. Diring, S. Furukawa, H. Uehara, T. Tsuruoka and S. Kitagawa, *J . Am. Chem. Soc.*, 2011, **133**, 15506; (d) T. Tsuruoka, S. Furukawa, Y. Takashima, K. Yoshida, S. Isoda and S. Kitagawa, *Angew. Chem. Int. Ed.*, 2009, **48**, 4739.

8 (a) M. Hu, J. S. Jiang, R. P. Ji and Y. Zeng, *CrystEngComm*, 2009, **11**, 2257; (b) M. Hu and Y. Yamauchi, *Chem. Asian J.*, 2011, **6**, 2282; (c) M. Hu, J. S. Jiang, C. C. Lin and Y. Zeng, *CrystEngComm*, 2010, **12**, 2679; (d) M. Hu, S. Ishihara, K. Ariga, M. Imura and Y. Yamauchi, *Chem. Eur. J.*, 2013, **19**, 1882; (e) L. Hu, P. Zhang, Q. Chen, H. Zhong, X. Hu, X. Zheng, Y. Wang and N. Yan, *Cryst. Growth Des.*, 2012, **12**, 2257; (f) F. X. Bu, C. J. Du, Q. H. Zhang and J. S. Jiang, *CrystEngComm*, 2014, **16**, 3113.

9 M. Hu and J. S. Jiang, *Mater. Res. Bull.*, 2011, **46**, 702.

10 (a) J. H. Her, P. W. Stephens, C. M. Kareis, J. G. Moore, K. S. Min, J.-W. Park, G. Bali, B. S. Kennon and J. S. Miller, *Inorg. Chem.*, 2010, **49**, 1524; (b) D. F. Shriver, S. A. Shriver and S. E. Anderson, *Inorg. Chem.*, 1965, **4**, 725.

11 R. E. Wilde, S. N. Ghosh and B. J. Marshall, *Inorg. Chem.*, 1970, **9**, 2512.

12 (a) H. Cölfen and M. Antonietti, *Angew. Chem. Int. Ed.*, 2005, **44**, 5576; (b) R. Q. Song and H. Cölfen, *Adv. Mater.*, 2010, **22**, 1301.

13 (a) L. Zhou and P. O'Brien, *J. Phys. Chem. Lett.*, 2012, **3**, 620; (b) J. Fang, B. Ding and H. Gleiter, *Chem. Soc. Rev.*, 2011, **40**, 5347.

14 (a) I. K. a. R. I. Kostov, *Pensoft Pulishers, Prof. Marin Drinov Academic Publishing House, Sofia,*, 1999, pp. 178 ; (b) T. Wang, M. Antonietti and H. Cölfen, *Chem. Eur. J.*, 2006, **12**, 5722; (c) B. Judat and M. Kind, *J. Colloid Interface Sci.*, 2004, **269**, 341; (d) Y. Ma, H. Cölfen and M. Antonietti, *J. Phys. Chem. B.*, 2006, **110**, 10822.

15 Y. Liu, W. Zhang, S. Li, C. Cui, J. Wu, H. Chen and F. Huo, *Chem. Mater.*, 2013, **26**, 1119.

16 S. R. Dickinson and K. M. McGrath, *J. Mater. Chem.*, 2003, **13**, 928.

17 (a) P. Zhao, J. Wang, G. Cheng and K. Huang, *J. Phys. Chem. B.*, 2006, **110**, 22400; (b) B. Qiu, Y. Ni and L. Zhang, *J. Cryst. Growth*, 2008, **310**, 4199; (c) K. Chen, S. Song and D. Xue, *J. Appl. Cryst.*, 2013, **46**, 1603.

18 M. Hu, J. S. Jiang and Y. Zeng, *Chem. Comm.*, 2010, **46**, 1133.

19 J. L. Wang and L. J. Xu, *Crit. Rev. Environ. Sci. Technol.*, 2011, **42**, 251.

20 (a) L. Gao, J. Zhuang, L. Nie, J. Zhang, Y. Zhang, N. Gu, T. Wang, J. Feng, D. Yang, S. Perrett and X. Yan, *Nature Nanotech.*, 2007, **2**, 577; (b) X. j. Yang, X. m. Xu, J. Xu and Y. f. Han, *J . Am. Chem. Soc.*, 2013, **135**, 16058.

21 T. Abe, F. Taguchi, S. Tokita and M. Kaneko, *J. Mol. Catal. A: Chem.*, 1997, **126**, L89.

22 R. Koncki, T. Lenarczuk and S. Glab, *Anal. Chim. Acta*, 2000, **424**, 27.

23 C. Nethravathi, C. R. Rajamathi, M. Rajamathi, X. Wang, U. K. Gautam, D. Golberg and Y. Bando, *ACS Nano*, 2014, **8**, 2755.

